Effect of Nonlinear Surface Interaction on Seismic Response of a Fracture

Aoife Toomey, Lawrence Berkeley National Laboratory, Christopher J. Bean, University College Dublin, and Oona Scotti, Institut de Protection et de Sûreté Nucléaire*

Summary

At the micro-scale a fracture consists of two rough surfaces in partial contact. The presence of void spaces between the asperities of contact on the fracture surfaces leads to increased deformability of the fracture, as a result of which fractures have a significant influence on the seismic wavefield. Field and laboratory experiments have shown that fractures have a frequency-dependent effect on the amplitudes and travel times of waves transmitted and reflected at the fracture and that a variety of interface waves can propagate along the fracture surfaces. The amplitudes and travel times of these events are strongly influenced by the fracture stiffness, which in turn depends on the fracture surface roughness and area of contact between the fracture surfaces. It may thus be possible to invert seismic data for not only the location but also the properties of fracture networks. Many fractures may exhibit nonlinear surface interaction when the confining pressure is low or when the dynamic strains are large. We investigate the effect of this nonlinearity on the seismic wavefield and demonstrate that seismic data can in theory, at low confining pressures or when the dynamic strains are high, be used to distinguish fracture tensile (cohesive) and compressional properties.

Introduction

Analytical models of fractures such as the displacement discontinuity model can predict the seismic response of a fracture as a function of its normal and shear *specific stiffnesses* and the incident wave frequency (Schoenberg, 1980; Pyrak-Nolte et al., 1990). Fracture normal *specific stiffness* is usually determined by subjecting the fracture to compression and measuring its deformation. Since a fracture's response to compression is a function only of the spatial geometry and mechanical properties of asperities on the fracture surfaces, these measurements neglect factors influencing the cohesive properties of the fracture - such as the degree of welding between the fracture surfaces. The fracture properties are assumed to be equal in compression and in tension, however, many fractures are obviously nonlinear since they have completely unwelded surfaces which can separate under tension (i.e. zero stiffness in tension). Fractures which have 'healed' may have nonzero tensile stiffnesses (cohesion). Fracture cohesion is of interest in many fields since it influences the fracture strength. Here, we present a particle-based numerical scheme capable of handling complex fracture geometries and distributions, as well as nonlinear fracture properties and heterogeneous stress fields. We propagate plane P waves across numerical fractures and investigate the effect of the fracture mechanical properties and confining pressure on the seismic wavefield.

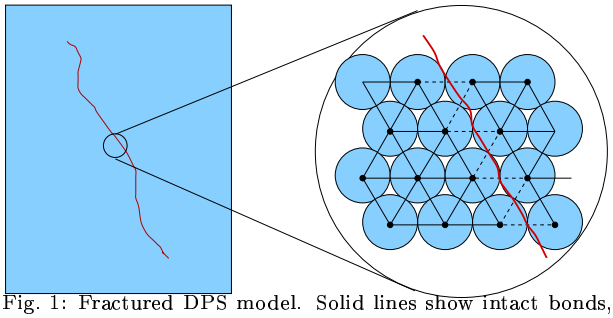

Fig. 1: Fractured DPS model. Solid lines show intact bonds, dashed lines show fractured bonds.

Particle-Based Modeling of Fractures

Particle-based methods approach rock deformation problems from the discrete, discontinuous perspective. Instead of solving differential equations describing the deformation process, these methods try to model the underlying physics of rock deformation which occur at some discrete scale (e.g. grain-scale interactions). Particles represent units of intact rock whose size depends on the desired application of the model and the available computational power.

The current implementation of the scheme, which we call the Discrete Particle Scheme (DPS), consists of a 2-D hexagonal arrangement of interacting particles. Particles interact at their contacts in accordance with Hooke's law:

$$F_{(i,j)} = K_{(i,j)}(r_{(i,j)} - r0_{(i,j)})\delta l \qquad (1)$$

This specifies the magnitude of the elastic force, F, acting between two neighbouring particles i and j as a result of deformation of the bond joining them, where $r_{(i,j)}$ is the distance between the particle centers, $K_{(i,j)}$ is the stiffness of the interparticle bond, $r0_{(i,j)}$ is the equilibrium spacing between the particles and δl is the particle thickness, which is always unity in the 2-D lattice. This model geometry results in a Poisson's ratio of $\frac{1}{4}$ for the medium. A complete description of the scheme for modelling intact rocks is given in Toomey and Bean (2000). The simple force-displacement interaction between the particles has been shown to capture wave propagation through intact heterogeneous media in accordance with continuum mechanics (Toomey and Bean, 2000) and allows us to model quasi-static rock deformation in accordance with linear elasticity theory (Toomey et al., 1999).

Seismic Response of a Nonlinear Fracture

Fractures are modelled in the DPS scheme as mechanical discontinuities of greater compliance than the surrounding material (figure1). The fracture's response to tensile and compressional stresses are governed by the fractured bond's tensile and compressional stiffnesses K^t_{bond} and K^c_{bond}:

$$F_{(i,j)} = \begin{cases} K^t_{bond_{(i,j)}}(r_{(i,j)} - r0_{(i,j)}) & r_{(i,j)} > r0_{(i,j)} \\ K^c_{bond_{(i,j)}}(r_{(i,j)} - r0_{(i,j)}) & r_{(i,j)} < r0_{(i,j)} \end{cases} \quad (2)$$

This modified Hooke's law allows us to capture nonlinear fracture surface interaction. $K^t_{bond_{(i,j)}}$ describes the cohesive properties of the fracture, and ranges between 0 for an unwelded fracture, and the stiffness of the host medium (in which case the rock is not fractured). $K^c_{bond_{(i,j)}}$ can have any non-zero value less than or equal to the stiffness of the intact rock (a 'perfectly' smooth fracture). Values of $K^c_{bond_{(i,j)}}$ lower than that of the intact rock capture the effects of surface roughness. This is an approximate approach and is less computationally expensive than explicitly modelling the surface roughness in the DPS. The particle diameter determines the length of the cross-fracture bonds and thus the width of the damaged zone. This fracture representation has been shown to capture the transmission and reflection of seismic waves at a fracture in accordance with the displacement discontinuity model (Toomey et al., 2002), as well as the generation and propagation of interface waves along the fracture surface (Toomey, 2001).

This numerical model offers advantages over analytical models of fractures due to the ease with which heterogeneous fracture geometries, as well as fracture nonlinearity, can be handled. Heterogeneous stress fields can also be modelled with ease.

In the following numerical experiments we used a model with the properties listed in table 1. These are representative of granite. The lateral boundary conditions are such that the model is effectively infinitely wide (reflections at the lateral boundaries are negligible). A fracture was located at the centre of the model and spanned its width. Examples of some of the fracture properties used are given in table 2. Normal *specific stiffnesses* of these fractures were measured both in compression and in tension, by applying a compressional or tensile stress across the fracture and measuring its resultant deformation. The *specific stiffness* is the ratio of applied stress to fracture deformation. Note that *specific stiffness* and *bond stiffness* are not the same. Plane P waves (continuous monochromatic sine waves with frequencies between 50 and 400 Hz) were propagated across the fracture. Plane wave propagation through the model is initiated by inputting a source function as a vertical displacement of the particles lining the lower boundary of the model. The seismic response of the fracture was then studied.

Unconfined Nonlinear Fracture

In these experiments we compared the seismic response

Young's modulus (GPa)	60.
P wave velocity (km/s)	5.2
S wave velocity (km/s)	3.
Density (kg/m^3)	2650.
Poisson's ratio	0.25
Intact bond stiffness (GPa)	55.43

Table 1: Properties of the numerical model used in these experiments. These properties are representative of granite.

	K^c_{bond}	K^t_{bond}	$K^c_{spec_n}$ (GPa/m)	$K^t_{spec_n}$ (GPa/m)
set 1	10%	10%	11.4	11.4
	20%	20%	25.6	25.6
	50%	50%	102.7	102.7
set 2	10%	5%	11.4	5.5
	20%	5%	25.6	5.5
	50%	5%	102.7	5.5

Table 2: Examples of some of the fracture properties used in the following experiments. K^c_{bond} and K^t_{bond} are the fracture bond compressional and tensile stiffnesses, respectively, as percentages of the intact rock bond stiffness. Normal *specific stiffnesses* were measured in compression ($K^c_{spec_n}$) and in tension ($K^t_{spec_n}$).

of linear ('set 1', table 2) and nonlinear ('set 2', table 2) fractures. As seen in figure 2, the transmitted and reflected waves produced by the set 2 fractures are asymmetrical, indicating that fracture tensile stiffness imparts a signature to the seismic wavefield. These fractures have two reflection coefficients - one for tensile wave pulses (which depends on its tensile stiffness) and another for compressional pulses (depending on its compressional stiffness). We measured the reflection and transmission coefficients of each fracture for tensile wave pulses ($|R|^t$ and $|T|^t$ respectively) by measuring the amplitude of the tensile component of the reflected and transmitted waves (figure 2). The coefficients of the fractures for compressional pulses ($|R|^c$ and $|T|^c$ respectively) were calculated from the amplitudes of the compressional components of the reflected and transmitted waves. As shown in figure 3, the coefficients calculated in this manner agree with those predicted from the displacement discontinuity theory, using the fracture normal *specific stiffness* measured **in compression** to calculate the coefficients for compressional wave pulses (figure 3 (a)) and the normal *specific stiffness* measured **in tension** to calculate the coefficients for tensile wave pulses (figure 3 (b)). The errors in these results are smaller than the symbols used in figure 3. These results suggest that tensile wave pulses propagated across fractures may be used to gain useful information about the degree of welding between the fracture surfaces. It should be noted that the nonlinearity of the set 2 fractures (equation 2) has resulted in the generation of harmonics in the transmitted and reflected waves which can be seen in figure 2 as a distortion of the wavefields. Harmonic generation is a signature of nonlinear wave propagation in damaged materials. This topic requires further investigation but allows us to suggest that this method may have applications in the study of nonlinear wave diagnostics of damage.

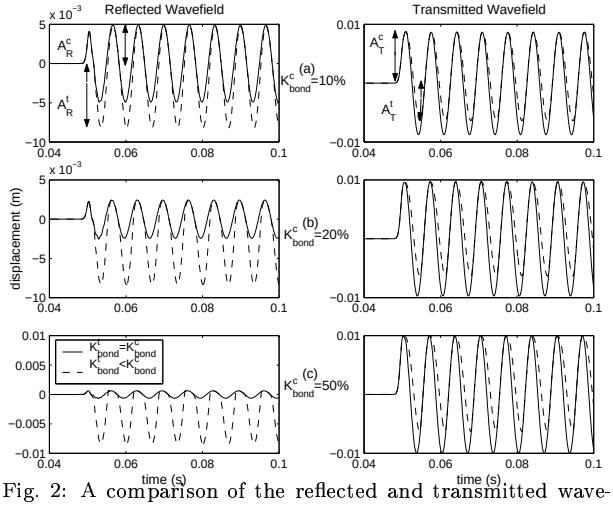

Fig. 2: A comparison of the reflected and transmitted wavefields produced by a 150 Hz plane P wave normally incident on set 1 (solid lines) and set 2 (dashed lines) fractures. 'Up' on these seismograms corresponds to compressional wave pulses, 'down' to tensile pulses. Amplitudes are normalised relative to the incident wave amplitude (i.e. they correspond to reflection/transmission coefficients).

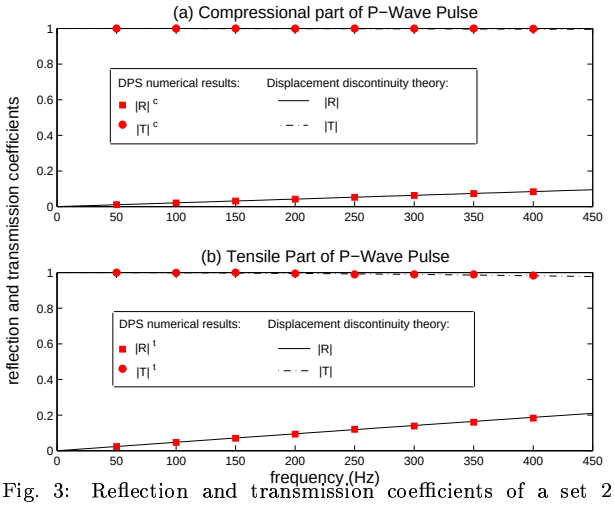

Fig. 3: Reflection and transmission coefficients of a set 2 fracture. Solid and dashed lines show the theoretical coefficients calculated based on the fracture's normal *specific stiffness* measured in compression (a) and in tension (b). Squares and circles show the coefficients measured in the DPS model, using the compressional components of the reflected and transmitted waves (a) and the tensile components of the reflected and transmitted waves (b).

Confined Nonlinear Fracture

We now investigate how the seismic response of nonlinear fractures varies with confining pressure. Real fractures have rough surfaces and increasing confining pressure on the fracture causes the surface contact area to increase, as a result of which the fracture stiffens and its seismic response changes. In these experiments we use perfectly smooth fractures so that the effects of nonlinearity in the fracture surface interaction can be isolated from those of surface roughness. The numerical model was subjected to vertical and horizontal stresses. We used values of 120 MPa for the maximum principal stress (this corresponds to a depth of approximately 4.5 km) and 10 MPa for the minimum principal stress (corresponding to a depth of approximately .5 km when this stress is vertical). Two experiments were carried out - first with the maximum principal stress acting normal to the fracture plane (case 1), then with the maximum stress acting parallel to the fracture plane (case 2). 50 Hz plane P waves were propagated across the confined fractures. We used a source displacement amplitude of .02 m.

Figure 4 compares reflected and transmitted P waves for cases 1 and 2. When the maximum principal stress acts normal to the fracture plane, the reflection and transmission coefficients of the fracture are found to be the same for tensile and compressional wave pulses, as for linear fractures. Both compressional and tensile wave pulses are in this case sampling the compressional properties of the fracture. Due to the large stress acting across the fracture, its surfaces are overlapping and the peak tensile displacement of the incident wavefield is not strong enough to take the fracture out of the compressional regime. When the orientation of the stress field is flipped, so that the stress acting across the fracture is 10 MPa and that acting parallel to it is 120 MPa, the fracture once again imparts an asymmetric signature to the wavefield. In this case the magnitude of the compressive strain across the fracture is lower than the dynamic strain associated with the incident wave. The fracture is still in the compressional regime for most of the time that it is excited by the incident wave. However, the tensile displacements of the incident wave are just strong enough to take it into the tensile regime. The tensile pulses are thus affected by both the tensile and compressional properties of the fracture, resulting in coefficients for tensile pulses that are a mixture of those given by the fracture compressional and tensile properties. We increased the magnitude of the minimum principal stress to 80 MPa, so that the fracture now has a 120 MPa stress acting along the fracture plane and an 80 MPa stress acting across it. In this case, the fracture's seismic signature reverts to that of a linear fracture , indicating that, even when the stress parallel to the fracture is greater than that perpendicular to it, the fracture surfaces overlap by an amount greater than the peak tensile displacement of the incident wave, and the fracture thus remains in the compressional regime throughout seismic

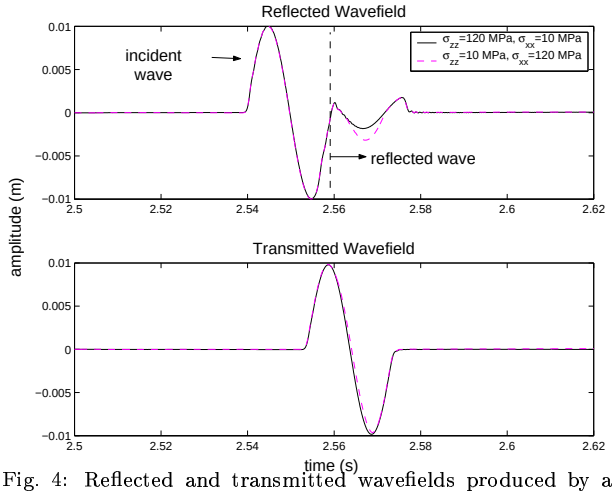

Fig. 4: Reflected and transmitted wavefields produced by a set 2 smooth fracture. Black solid lines show the results for a model compressed normal to the fracture plane by 120 MPa and parallel to the fracture by 10 MPa. Pink dashed lines show results for a normal stress of 10 MPa and a parallel stress of 120 MPa.

excitation. Since the source amplitude used in these experiments results in strains many times those associated with earthquake and controlled-source seismology, it is expected that even for low fracture-normal stresses, only the compressional properties of a smooth fracture would be sampled by a seismic wave.

Conclusions

Our results show that nonlinear fractures impart a characteristic signature to the wavefield. This result may be of importance in laboratory studies of fracture properties, as it suggests that seismic data may be inverted for both the cohesive and compressional properties of fractures. When confining pressures are applied to the fracture, only very large dynamic strains sample the fracture cohesive properties, as the fracture resides in the compressional regime. This suggests that the cohesive properties of fractures in the crust have no effect on seismic waves of earthquake or controlled-source origin. However, real fractures are rough and have aperture. Brown & Scholz (1985) have shown that, even at normal loads up to 50 MPa (equivalent to 1.7 km depth), less than 1% of a fracture's surfaces are in contact. Borehole televiewer images have provided further evidence that faults can be open and hydraulically conductive at these stresses (Townend and Zoback, 2000). Further work will incorporate more realistic fracture geometries (self-affine surface roughness) and dynamic stress fields similar to those associated with earthquake or exploration seismology, to determine whether this effect persists for dynamically illuminated fractures in crustal conditions.

Acknowledgements

The authors would like to thank Kurt Nihei and Seiji Nakagawa for valuable comments and suggestions.

References

Pyrak-Nolte, L. J., Myer, L. R., and Cook, N. G. W., 1990, Transmission of seismic waves across single natural fractures: Journal of Geophysical Research, **95**, no. B6, 8617–8638.

Schoenberg, M., 1980, Elastic wave behaviour across linear slip interfaces: Journal of the Acoustical Society of America, **68**, 1516–1521.

Toomey, A., and Bean, C., 2000, Numerical simulation of seismic waves using a discrete particle scheme: Geophysical Journal International, **141**, 595–604.

Toomey, A., Bean, C., Scotti, O., and Volant, P., 1999, Discrete particle simulations of seismic wave propagation through fractured media: Proceedings - AGU Fall Meeting, **80**, no. 46, 745.

Toomey, A., Bean, C., and Scotti, O., 2002, Fracture properties from seismic data - a numerical investigation: Geophysical Research Letters, **29**, no. 4.

Toomey, A., 2001, Particle-based numerical modelling of seismic wave propagation in fractured rock: Ph.D. thesis, University College Dublin, Ireland.

Townend, J., and Zoback, M. D., 2000, How faulting keeps the crust strong: Geology, **28**, no. 5, 399–402.